Transmitter-Side Wireless Information- and Power-Transfer in Massive MIMO Systems

A. A. Nasir[1], H. D. Tuan[2], T. Q. Duong[3] and L. Hanzo[4]

***Abstract*—Both time-switching (TS) and power splitting has been used at the receiver for wireless information and power transfer in the downlink of massive multiple-input-multiple-output systems. By contrast, this correspondence adopts the transmit-TS approach, where the energy and information are transferred over different fractions of a time slot. Our goal is to jointly optimize the transmit-TS factor and power allocation coefficients during energy and information transfer for maximizing the users' minimum throughput subject to transmit power and minimum harvested energy constraints. This nonconvex problem is solved by our path following algorithm. Our simulation results demonstrate the benefits of the proposed transmit-TS algorithm, which easily doubles the throughput compared to that of the existing techniques.**

***Index Terms*—Beamforming, massive MIMO, wireless power transfer**

I. Introduction

Wireless power transfer (WPT) is a promising energy harvesting technique conceived for extending the battery-recharge period of energy-constrained nodes in wireless networks [1], [2]. Hence WPT relying on massive multiple-input-multiple-output (m-MIMO) systems has been considered in the specific contexts of both space-division multiple access (SDMA) [3]–[5] as well as in power splitting (PS) [6]–[8] and time switching (TS) [9]. The SDMA solution relies on the transfer of energy and information over different beam directions [10]. In the PS approach, information and energy are simultaneously transmitted using the same signal by the BS. At the receiver, a power splitter is employed for partitioning the received signal into a component for information decoding and another for energy harvesting (EH) [11]. The conventional TS approach can be referred to as a "receive-TS" approach, where instead of the power splitter used at the receiver, a time switch is applied to the received signal, allowing the UE to decode the information during a certain fraction of time and then harvest energy in the remaining time. In general, the PS approach outperforms the receive-TS technique [9] but the former is not very practical, since it requires a variable power-splitter.

Our previous treatise [12] introduced the "transmit-TS" approach, where information and energy are sent over different time-fractions within a time slot. The architecture of the receive-TS and transmit-TS approaches is illustrated in Figs. 1 and 2, respectively. Instead of transmitting a signal $\mathbf{x}$ (the dimension of the vector is given by the antenna-array size) over the whole slot duration T, as in the receive-TS approach, the transmit-TS approach conveys a separate energy signal $\mathbf{x}_{\rm E}$ and an information signal $\mathbf{x}_{\rm I}$ over different time-fractions, $t_{\rm E}$ and $t_{\rm I}$ of the time slot, respectively. As a result, the EH receiver and information receiver of the transmit-TS technique processes the pair of received signals, $y_{{\rm E},n}$ and $y_{{\rm I},n}$, respectively. This is in contrast to the receive-TS approach, where the same received signal y_n is processed by both the receivers to harvest energy and to decode the information. The diversity of sending different signals over different time-fractions within a TS helps the transmit-TS approach to outperform the conventional receive-TS approach [12].

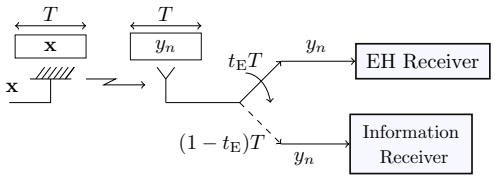

Fig. 1: Conventional receive-TS architecture.

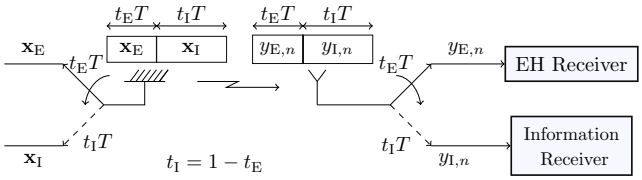

Fig. 2: Transmit TS architecture.

For m-MIMO systems, the unstructured beamforming design of [12] becomes a computationally intractable excessive-dimensional nonconvex problem. In a m-MIMO context the TS approach of [13] may be deemed reminiscent of the transmit-TS approach, but the challenge of jointly optimizing the TS factor and the power allocation coefficients was not tackled. Hence we solve this open research challenge. Furthermore, in [9], [13] conjugate beamforming (CB) was used, which is quite efficient for WPT, but not for information transfer [14].

For a modest number of antennas at the BS, the transmit-TS approach outperformed both the receive-TS and the PS approaches [12], [15]. However, its extension to m-MIMO systems has hitherto not been considered due to the computational complexity of the corresponding optimization problem, which became large-scale nonconvex. This

[1]Department of Electrical Engineering, King Fahd University of Petroleum and Minerals (KFUPM), Dhahran, Saudi Arabia (e-mail: anasir@kfupm.edu.sa); [2]School of Electrical and Data Engineering, University of Technology Sydney, Broadway, NSW 2007, Australia (e-mail: tuan.hoang@uts.edu.au); [3] Queen's University Belfast, Belfast BT7 1NN, UK (email: trung.q.duong@qub.ac.uk); [4]School of Electronics and Computer Science, University of Southampton, Southampton, SO17 1BJ, U.K. (e-mail: lh@ecs.soton.ac.uk).

correspondence aims to fill the gap by opting for structured beamforming. The transmit-TS approach facilitates the use of CB for efficient power transfer and then zero forcing ZF beamforming (ZFB) for efficient information transfer. The optimization task is to jointly optimize the transmit-TS factor and the power allocation coefficients during energy and information transfer for maximizing the users' minimum rate subject to minimum harvested energy constraint. To solve this nonconvex problem, we propose a novel path following algorithm for its computation. We will demonstrate that the proposed transmit-TS algorithm achieves a clear performance gain over the existing techniques for wireless power and information transfer in massive MIMO systems.

Notation: Bold-faced upper-case letters, e.g., $\mathbf{X}$, are used for matrices, bold-faced lower-case letters, e.g., $\mathbf{x}$, are used for vectors, and lower-case letters, e.g., x, are used for scalars. $\mathbf{x}^H$, $\mathbf{x}^T$, and $\mathbf{x}^*$ denote Hermitian transpose, normal transpose, and conjugate of the vector $\mathbf{x}$, respectively. $\|\cdot\|$ stands for the vector's Euclidean norm and $|\cdot|$ denotes the absolute value of a scalar number. $\mathbb{C}$ is the set of all complex numbers and $\mathbb{E}$ is the expectation operator. $\mathbf{I}_N$ denotes the identity matrix of size $N \times N$. For $\mathbf{x} \geq 0$ for $\mathbf{x} = (x_1, \ldots, x_n)^T$ is entry-wise understood, i.e. $x_i \geq 0$ for $i = 1, \ldots, n$.

II. System Model and Problem Formulation

Let us consider the downlink communication of an M-antenna aided BS serving N single-antenna users. The user set $\mathcal{N} \triangleq \{1, \ldots, N\}$ can be divided into two zones where N_1 users are located close to the BS, while the remaining $N_2 = N - N_1$ users are outside this zone. The nearby users $n \in \mathcal{N}_1 \triangleq \{1, \ldots, N_1\}$, are capable of both information decoding and energy harvesting, while the distant users only process information. It is not only more general but also more viable to consider that all users expect information from the BS, while the energy-constrained users in the vicinity of the BS exploit the opportunity to replenish their battery. Under the transmit-TS approach [12], a fraction of time $0 < t_{\mathrm{E}} < 1$ is used for power transfer while the remaining fraction of time $t_{\mathrm{I}} = 1 - t_{\mathrm{E}}$ for information transfer. The channel spanning from the BS to user n is modelled by $\sqrt{\beta_n}\mathbf{h}_n^H$, where $\sqrt{\beta_n}$ models the path-loss and large-scale fading, $\mathbf{h}_n = \mathbf{\Theta}_n^{1/2}\tilde{\mathbf{h}}_n \in \mathbb{C}^{M\times 1}$ is the channel vector from the BS to the user n, so that $\mathbf{\Theta}_n \in \mathbb{C}^{M\times M}$ is a Hermitian symmetric positive semidefinite spatial correlation matrix, and $\tilde{\mathbf{h}}_n \in \mathbb{C}^{M\times 1}$ is a normalized small-scale fading channel. Channel information can be acquired by exploiting the channel reciprocity [9], [16], but this is beyond the scope of this work as we focus on downlink communication and on efficient wireless information and power transfer in a m-MIMO system.

Energy transfer by CB: The signal received by user $n \in \mathcal{N}_1$ during the energy transfer period t_{E} is given by

$$y_{\mathrm{E},n} = \sqrt{\beta_n}\mathbf{h}_n^H \mathbf{x}_{\mathrm{E}} + v_n, \tag{1}$$

where v_n is the independent and identically distributed (i.i.d.) additive white Gaussian noise with zero mean as well as variance σ^2, and $\mathbf{x}_{\mathrm{E}} = \sum_{n=1}^{N_1}\sqrt{p_{\mathrm{E},n}}\mathbf{h}_n s_{\mathrm{E},n}$ is the energy signal transmitted to the nearby users, which is composed of N_1 independent energy symbols $s_{\mathrm{E},n}$ with $\mathbb{E}(|s_{\mathrm{E},n}|^2) = 1$, and each $p_{\mathrm{E},n}$ is the power allocated to the conjugate beamformer $\mathbf{h}_n$. For the vector of power allocation $\mathbf{p}_{\mathrm{E}} \triangleq [p_{\mathrm{E},1}, p_{\mathrm{E},2}, \ldots, p_{\mathrm{E},N_1}]^T$, the energy harvested by user $n \in \mathcal{N}_1$, assuming a linear EH model, which is given by $t_{\mathrm{E}}E_n(\mathbf{p}_{\mathrm{E}})$, where

$$E_n(\mathbf{p}_{\mathrm{E}}) \triangleq \eta\beta_n \sum_{n'=1}^{N_1} p_{\mathrm{E},n'} \left|\mathbf{h}_n^H \mathbf{h}_{n'}\right|^2. \tag{2}$$

for the energy conversion efficiency $0 < \eta < 1$.[1]

Information Transfer by ZFB: The signal received by user $n \in \mathcal{N}$ during the *information* transfer period $t_{\mathrm{I}} = 1 - t_{\mathrm{E}}$ is given by

$$y_{\mathrm{I},n} = \sqrt{\beta_n}\mathbf{h}_n^H \mathbf{x}_{\mathrm{I}} + v_n, \tag{3}$$

where $\mathbf{x}_{\mathrm{I}} \in \mathbb{C}^{M\times 1}$ is the composite information signal transmitted to all N users, which is given by

$$\mathbf{x}_{\mathrm{I}} = \mathbf{W}_{\mathrm{I}}\mathsf{diag}\left(\sqrt{\mathbf{p}_{\mathrm{I}}}\right)\mathbf{s}_{\mathrm{I}},$$

where $\mathbf{W}_{\mathrm{I}} \triangleq [\mathbf{w}_{\mathrm{I},1}, \ldots, \mathbf{w}_{\mathrm{I},N}] = \mathbf{H}\left(\mathbf{H}^H\mathbf{H}\right)^{-1}$ for $\mathbf{H} \triangleq [\mathbf{h}_1, \ldots, \mathbf{h}_N]$, $\mathbf{s}_{\mathrm{I}} \triangleq [s_{\mathrm{I},1}, s_{\mathrm{I},2}, \ldots, s_{\mathrm{I},N}]^T$ is the vector of information symbols transmitted to the N users with $\mathbb{E}\left[\mathbf{s}_{\mathrm{I}}\mathbf{s}_{\mathrm{I}}^H\right] = \mathbf{I}_N$, and $\mathbf{p}_{\mathrm{I}} \triangleq [p_{\mathrm{I},1}, p_{\mathrm{I},2}, \ldots, p_{\mathrm{I},N}]^T$ is the vector of power allocation. The throughput under ZF beamforming is given by

$$r_n(p_{\mathrm{I},n}, t_{\mathrm{I}}) = t_{\mathrm{I}} \ln\left(1 + p_{\mathrm{I},n}/\mathcal{L}_n\right), \tag{4}$$

where $\mathcal{L}_n \triangleq \sigma^2/\left(\left|\mathbf{h}_n^H\mathbf{w}_{\mathrm{I},n}\right|^2\beta_n\right)$.

Problem Formulation: We aim to solve the following problem of max-min throughput optimization problem under EH and total power constraints:

$$\max_{\{\mathbf{p}_{\mathrm{I}}, \mathbf{p}_{\mathrm{E}}, t_{\mathrm{E}}, t_{\mathrm{I}}\}} \min_{n=1,\ldots,N} r_n(\mathbf{p}_{\mathrm{I}}, t_{\mathrm{I}}) \tag{5a}$$

$$\text{s.t. } E_n(\mathbf{p}_{\mathrm{E}}) \geq e_n^{\min}/t_{\mathrm{E}},\ n \in \mathcal{N}_1, \tag{5b}$$

$$\sum_{\mathcal{S}\in\{\mathrm{I},\mathrm{E}\}} t_{\mathcal{S}}\varphi_{\mathcal{S}}(\mathbf{p}_{\mathcal{S}}) \leq P_T, \tag{5c}$$

$$\mathbf{p}_{\mathrm{I}} \geq 0, \mathbf{p}_{\mathrm{E}} \geq 0, 0 < t_{\mathrm{I}}, 0 < t_{\mathrm{E}}, t_{\mathrm{I}} + t_{\mathrm{E}} = 1, \tag{5d}$$

where $e_n^{\min}$ is the EH threshold and (8b) represents the total power constraint with $\varphi_{\mathrm{I}}(\mathbf{p}_{\mathrm{I}}) \triangleq \sum_{n=1}^{N}\|\mathbf{w}_{\mathrm{I},n}\|^2 p_{\mathrm{I},n}$ and $\varphi_{\mathrm{E}}(\mathbf{p}_{\mathrm{E}}) \triangleq \sum_{n=1}^{N_1}\|\mathbf{h}_n\|^2 p_{\mathrm{E},n}$.

Lemma 1: At the optimal solution $(\mathbf{p}_{\mathrm{I}}^{opt}, \mathbf{p}_{\mathrm{E}}^{\mathrm{opt}}, t_{\mathrm{E}}^{\mathrm{opt}}, t_{\mathrm{I}}^{\mathrm{opt}})$ of (5) the rates are balanced, i.e.

$$p_{I,1}^{\mathrm{opt}}/\mathcal{L}_1 = p_{I,n}^{\mathrm{opt}}/\mathcal{L}_n, n = 2, \ldots, N. \tag{6}$$

Proof: See the Appendix A. □

[1]The use of non-linear EH model is beyond the scope of this work and can be the subject of future research.

By Lemma 1, we seek $\mathbf{p}_I$ in the following class

$$p_{\mathrm{I},n}/\mathcal{L}_n = p_{\mathrm{I},1}/\mathcal{L}_1, n = 2, \ldots, N$$
$$\Leftrightarrow \quad p_{\mathrm{I},n} = \frac{\beta_1 \left|\mathbf{h}_1^H \mathbf{w}_{\mathrm{I},1}\right|^2}{\beta_n \left|\mathbf{h}_n^H \mathbf{w}_{\mathrm{I},n}\right|^2} p_{\mathrm{I},1}, n = 2, \ldots, N. \quad (7)$$

Under (7), (5) is equivalently simplified to

$$\max_{\mathbf{v} \triangleq \{p_{\mathrm{I},1}, \mathbf{p}_{\mathrm{E}}, t_{\mathrm{E}}, t_{\mathrm{I}}\}} \Phi(\mathbf{v}) \triangleq r_1(p_{\mathrm{I},1}, t_{\mathrm{I}}) \quad \text{s.t.} \quad (5b), (5d), \quad (8a)$$
$$\xi t_{\mathrm{I}} p_{\mathrm{I},1} + t_{\mathrm{E}} \varphi(\mathbf{p}_{\mathrm{E}}) \leq P_T, \quad (8b)$$
$$p_{\mathrm{I},1} \geq 0, \mathbf{p}_{\mathrm{E}} \geq 0, \quad (8c)$$

where $\xi \triangleq \|\mathbf{w}_{\mathrm{I},1}\|^2 + \sum_{n=2}^{N} \frac{p_{\mathrm{I},n}}{p_{\mathrm{I},1}} \|\mathbf{w}_{\mathrm{I},n}\|^2] = \|\mathbf{w}_{\mathrm{I},1}\|^2 + \sum_{n=2}^{N} \frac{\beta_1 \left|\mathbf{h}_1^H \mathbf{w}_{\mathrm{I},1}\right|^2}{\beta_n \left|\mathbf{h}_n^H \mathbf{w}_{\mathrm{I},n}\right|^2} \|\mathbf{w}_{\mathrm{I},n}\|^2$. It is important to mention that both problems (5) and (8) result in the same solution however, the latter involves only single information power variable $p_{\mathrm{I},1}$. Due to the non-concave objective function (8a) and the nonconvex constraint (8b), the problem (8) is nonconvex. The problem is bit more complex due to the product of optimization variables in (8a) and (8b).

III. Proposed Algorithm

Let $\mathbf{v}^{(\kappa)} \triangleq \{p_{\mathrm{I},1}^{(\kappa)}, \mathbf{p}_{\mathrm{E}}^{(\kappa)}, t_{\mathrm{I}}^{(\kappa)}, t_{\mathrm{E}}^{(\kappa)}\}$ with $\mathbf{p}_{\mathrm{E}}^{(\kappa)} \triangleq \left[p_{\mathrm{E},1}^{(\kappa)}, \cdots, p_{\mathrm{E},N_1}^{(\kappa)}\right]^T$ be the feasible point for (8) that is found from the $(\kappa-1)$th iteration.

Let us start by finding a lower bounding concave approximation of the objective function in (8a). Applying the inequality (20) in the Appendix B for $x = p_{\mathrm{I},1}/\mathcal{L}_1$ and $\bar{x} = p_{\mathrm{I},1}^{(\kappa)}/\mathcal{L}_1$ gives

$$r_1(p_{\mathrm{I},1}, t_{\mathrm{I}}) \geq r_1^{(\kappa)}(p_{\mathrm{I},1}, t_{\mathrm{I}}) \triangleq a_1^{(\kappa)} - \frac{b_1^{(\kappa)}}{t_{\mathrm{I}}} - \frac{c_1^{(\kappa)}}{p_{\mathrm{I},1}} \quad (9)$$

for $a_1^{(\kappa)} = 2r_1(p_{\mathrm{I},1}^{(\kappa)}, t_{\mathrm{I}}^{(\kappa)}) + f_1^{(\kappa)}$, $0 < b_1^{(\kappa)} = r_1(p_{\mathrm{I},1}^{(\kappa)}, t_{\mathrm{I}}^{(\kappa)}) t_{\mathrm{I}}^{(\kappa)}$, $c_1^{(\kappa)} = f_1^{(\kappa)} p_{\mathrm{I},1}^{(\kappa)}$, and $0 < f_1^{(\kappa)} = p_{\mathrm{I},1}^{(\kappa)} t_{\mathrm{I}}^{(\kappa)} / (\mathcal{L}_1 + p_{\mathrm{I},1}^{(\kappa)})$.

Next, we find the following inner approximation of the power constraint (8b) by using (21):

$$\frac{\xi t_{\mathrm{I}}^{(\kappa)} p_{\mathrm{I},1}^{(\kappa)}}{4} \left(\frac{t_{\mathrm{I}}}{t_{\mathrm{I}}^{(\kappa)}} + \frac{p_{\mathrm{I},1}}{p_{\mathrm{I},1}^{(\kappa)}} \right)^2 + \frac{t_{\mathrm{E}}^{(\kappa)} \varphi(\mathbf{p}_{\mathrm{E}}^{(\kappa)})}{4} \left(\frac{t_{\mathrm{E}}}{t_{\mathrm{E}}^{(\kappa)}} + \frac{\varphi(\mathbf{p}_{\mathrm{E}})}{\varphi(\mathbf{p}_{\mathrm{E}}^{(\kappa)})} \right)^2 \leq P_T. \quad (10)$$

At the κth iteration, we solve the following convex optimization problem of polynomial computational complexity $\mathcal{O}\big((N_1+3)^3(2N_1+5)\big)$ [17, p. 4] for generating the next feasible point $\mathbf{v}^{(\kappa+1)} \triangleq \{p_{\mathrm{I},1}^{(\kappa+1)}, \mathbf{p}_{\mathrm{E}}^{(\kappa+1)}, t_{\mathrm{E}}^{(\kappa+1)}, t_{\mathrm{I}}^{(\kappa+1)}\}$ for (8)

$$\max_{\mathbf{v}} \ \Phi^{(\kappa)}(\mathbf{v}) \triangleq r_1^{(\kappa)}(p_{\mathrm{I},1}, t_{\mathrm{I}}) \text{ s.t. } (5b), (5d), (8c), (10). \quad (11)$$

Algorithm 1 summarizes the associated computational procedure, which iteratively solves the convex problem (11). The initial feasible solution can be obtained by assuming $t_{\mathrm{I}}^{(0)} = t_{\mathrm{I}}^{(0)} = 0.5$ and then solving for the resultant convex constraints (5b) and (8b) under fixed $t_{\mathrm{I}}^{(0)} = t_{\mathrm{I}}^{(0)} = 0.5$.

Algorithm 1 Path-following algorithm for solving the problem (8)

1: **Initialization**: Take any feasible initial point $\mathbf{v}^{(0)} \triangleq \{p_{\mathrm{I},1}^{(0)}, \mathbf{p}_{\mathrm{E}}^{(0)}, t_{\mathrm{E}}^{(0)}, t_{\mathrm{I}}^{(0)}\}$ of the problem (8). Set $\kappa = 0$.
2: **Repeat until convergence of the objective function in** (8): Solve the convex problem (11) to generate $\mathbf{v}^{(\kappa+1)}$. Set $\kappa \to \kappa + 1$.

Note that we have $\Phi^{(\kappa)}(\mathbf{v}^{(\kappa+1)}) > \Phi^{(\kappa)}(\mathbf{v}^{(\kappa)})$ provided that $\mathbf{v}^{(\kappa+1)} \neq \mathbf{v}^{(\kappa)}$ holds because the latter and the former represent a feasible point and the optimal solution of (11), respectively. Therefore we have $\Phi(\mathbf{v}^{(\kappa+1)}) \geq \Phi^{(\kappa)}(\mathbf{v}^{(\kappa+1)}) > \Phi^{(\kappa)}(\mathbf{v}^{(\kappa)}) = \Phi(\mathbf{v}^{(\kappa)})$, i.e. $\mathbf{v}^{(\kappa+1)}$ is a better feasible point for (8) than $\mathbf{v}^{(\kappa)}$. As such, Algorithm 1 generates a sequence of improved-feasibility points for (8) and converges at least to a locally optimal solution of (8) [18].

Remark 1: In order to see the benefit of optimizing the transmit-TS time, t_{E} or t_{I}, the next section will compare its performance to that of the "transmit-TS with fixed t_{E}" approach. This approach does not optimize t_{E}, but fixes $t_{\mathrm{E}}^{\mathrm{fix}} = 0.5$, under which the problem (8) is decomposed into the problem of power allocation during energy transfer and the information transfer time-durations. The optimal power allocation vector $\mathbf{p}_{\mathrm{E}}^{opt}$ is found as the optimal solution of the following linear problem:

$$\min_{\mathbf{p}_{\mathrm{E}} \geq 0} \ \varphi_{\mathrm{E}}(\mathbf{p}_{\mathrm{E}}) \triangleq \sum_{n=1}^{N_1} \|\mathbf{h}_n\|^2 p_{\mathrm{E},n} \quad (12a)$$
$$\text{s.t.} \quad E_n(\mathbf{p}_{\mathrm{E}}) \geq e_n^{\min}/t_{\mathrm{E}}^{\mathrm{fix}}, \ n \in \mathcal{N}_1, \quad (12b)$$

while the power allocation $p_{\mathrm{I},1}^{opt}$ is

$$p_{\mathrm{I},1}^{opt} = \frac{P_T - t_{\mathrm{E}}^{\mathrm{fix}} \varphi(\mathbf{p}_{\mathrm{E}}^{opt})}{\xi \left(1 - t_{\mathrm{E}}^{\mathrm{fix}}\right)}, \quad (13)$$

which is the optimal solution of the problem

$$\max_{p_{\mathrm{I},1} \geq 0} \ \left(1 - t_{\mathrm{E}}^{\mathrm{fix}}\right) \ln\left(1 + p_{\mathrm{I},1}/\mathcal{L}_1\right) \quad (14a)$$
$$\text{s.t. } \xi \left(1 - t_{\mathrm{E}}^{\mathrm{fix}}\right) p_{\mathrm{I},1} + t_{\mathrm{E}}^{\mathrm{fix}} \varphi_{\mathrm{E}}(\mathbf{p}_{\mathrm{E}}^{opt}) \leq P_T. \quad (14b)$$

IV. Numerical Simulations

This section evaluates the performance of the proposed algorithm by numerical examples at $P_T = 16$ dBW for the transmit power budget, $e_n^{\min} \equiv e^{\min} = -20$ dBm for the energy harvesting threshold and $\eta = 0.5$ for the energy harvesting conversion efficiency. Unless stated otherwise, the number of antennas at the BS is $M = 100$ and the number of users is $N = 20$. All users are uniformly distributed on a circle of radius 300 m, where the $N_1 = 5$ nearby users, who perform both energy harvesting and information decoding, are located within the radius of

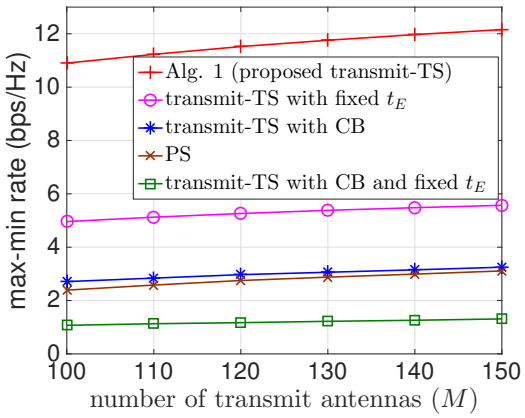

Fig. 3: Max-min rate performance versus M.

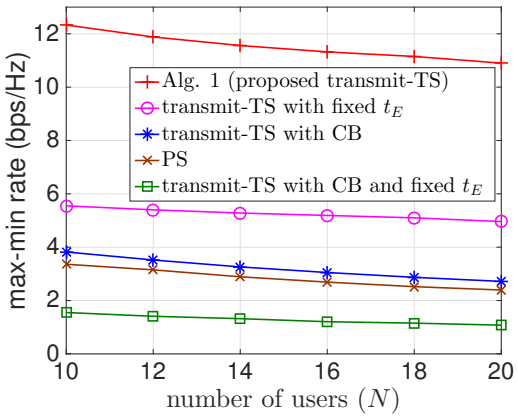

Fig. 4: Max-min rate performance versus N.

50 meters. The remaining $N_2 = (N - N_1)$ users are uniformly distributed on a disc with the inner radius of 50 m and the outer radius of 300 m. Following the channel model of [19], the large scale fading coefficient is given by $\beta_n = -30 - 10\gamma_n \log_{10}(d_n)$ (in dB), where γ_n, which is 3 for $n \in \mathcal{N}_1$ and 3.76 for $\mathcal{N} \setminus \mathcal{N}_1$, is the path-loss exponent and d_n is the distance of UE n from the BS. The normalized small-scale fading channel $\tilde{\mathbf{h}}_n$ follows Rayleigh distribution, except for $n \in \mathcal{N}_1$, obeys Rician distribution with a Rician K-factor of 10 dB. The BS is equipped with a uniform linear array of half-wavelength antenna-spacing [20]. To investigate the impact of the channel's spatial correlation, we adopt the correlated Rayleigh fading model of [19], [20, Sec. 2.6], where the covariance matrix is modeled by the Gaussian local scattering model

$$[\mathbf{\Theta}_n]_{p,q} = \frac{1}{L}\sum_{\ell=1}^{L} e^{\pi(p-q)\sin(\phi_n^\ell)} e^{-\frac{\sigma_\phi^2}{2}[\pi(p-q)\cos(\phi_n^\ell)]^2}, \quad (15)$$

where the number of scattering clusters is $L = 6$, the nominal angle of arrival (AoA) for the nth cluster and the angular standard deviation are $\phi_n^\ell \sim \mathcal{U}[\phi_n - 40^\circ, \phi_n + 40^\circ]$ and $\sigma_\phi = 5^\circ$, respectively. In order to investigate the performance of the proposed Alg. 1 in detail, we compare its performance to that of the following techniques:

- *transmit-TS with fixed t_E*, which refers to the transmit-TS approach with fixed $t_{\mathrm{E}} = 0.5$;
- *transmit-TS with CB and fixed t_E*, which refers to the transmit-TS approach with fixed $t_{\mathrm{E}} = 0.5$. Moreover, instead of ZFB, it assumes CB for information transfer, i.e., $\mathbf{w}_{\mathrm{I},n} = \mathbf{h}_n$, for $n \in \mathcal{N}$;
- *transmit-TS with CB*, which refers to the transmit-TS approach with CB instead of ZFB;
- *PS*, which refers to the PS approach [6], [7], [9], [13].

Among [6], [7], [9], [13], only [9] considered the problem of minimum-user rate optimization with using an approximation upon large M for computational ease. We do not compare the results with the conventional receive-TS approach because it has been shown in general that it is outperformed by the PS approach [9]. Therefore, our results show the comparison with the better PS approach.

Figs. 3 and 4 plot the optimized max-min rate versus the number of transmit antennas M and the number of users N, respectively. Fig 3 shows that the max-min user rate gracefully increases upon increasing M due to the availability of more resources and degrees of freedom.

Fig. 4 shows that the max-min user-rate slightly decreases with the increase in N, because the number of users competing for the fixed resources is increasing. Figs. 3 and 4 clearly show the performance gain of the proposed transmit-TS algorithm, which easily doubles the throughput compared to that of the existing techniques. Fig. 3 also shows the importance of joint optimization of t_{E} along with the power coefficients and the choice of beamformers, because with fixed t_{E} (as adpoted in [13]) and the CB for information transfer (as adpoted in [9], [13]), there is almost no improvement in the max-min user rate upon increasing the number of antennas.

The average EH time t_{E} for the proposed Alg. 1 versus the number of transmit antennas M is shown in Table I. As expected, the EH time decreases with the increase in M, because less time will be required for harvesting the threshold energy in the presence of more transmit antennas. Under $M = 150$ antennas , $N = 20$ users and $N_1 = 5$ nearby users, the Alg. 1 just takes around 15 iterations, on average, to converge.

TABLE I: Average EH time t_{E} for the proposed Alg. 1 versus the number of transmit antennas M

M	100	110	120	130	140
$t_{\mathrm{E}} \times 100\%$	1.85%	1.65%	1.48%	1.36%	1.28%

V. Conclusions

The transmit-TS technique of simultaneously supporting both wireless information and power transfer in the downlink of a massive MIMO system has been adopted. The

main challenge was the joint optimization of the transmit-TS factor and the power allocation coefficients during energy and information transfer to maximize the users' minimum rate subject to the EH constraint. This nonconvex problem has been addressed by means of a novel path following algorithm. The simulation results have shown the merits of the proposed algorithm over the existing techniques.

APPENDIX A: THE PROOF OF LEMMA 1

Let us assume by contradiction that (6) is not true. Without loss of generality we can have

$$p_{\mathrm{I},1}^{\mathrm{opt}}/\mathcal{L}_1 = \min_{n=1,\ldots,N} p_{\mathrm{I},n}^{\mathrm{opt}}/\mathcal{L}_n \quad (16)$$

$$< p_{\mathrm{I},N}^{\mathrm{opt}}/\mathcal{L}_N = \max_{n=1,\ldots,N} p_{\mathrm{I},n}^{\mathrm{opt}}/\mathcal{L}_n, \quad (17)$$

and thus there is $\epsilon > 0$ such that

$$p_{\mathrm{I},1}^{\mathrm{opt}}/\mathcal{L}_1 \leq p_{\mathrm{I},n}^{\mathrm{opt}}/\mathcal{L}_n - \epsilon, n = 2, \ldots, N, \quad (18)$$

and

$$p_{\mathrm{I},N}^{\mathrm{opt}}/\mathcal{L}_N \geq p_{\mathrm{I},n}^{\mathrm{opt}}/\mathcal{L}_n + \epsilon, n = 1, \ldots, N-1. \quad (19)$$

Taking $0 < \epsilon_1$ and $0 < \epsilon_N$ such that

$$\epsilon_1/\mathcal{L}_1 < \epsilon/2$$

and

$$\epsilon_N/\mathcal{L}_N < \min\{\epsilon/2, p_{\mathrm{I},N}^{\mathrm{opt}}\}$$

with

$$\epsilon_1 ||\mathbf{w}_1||^2 \leq \epsilon_N ||\mathbf{w}_N||^2$$

to obtain $\bar{\mathbf{p}}_{\mathrm{I}} \triangleq [p_{\mathrm{I},1}^{\mathrm{opt}} + \epsilon_1, p_{\mathrm{I},2}^{\mathrm{opt}}, \ldots, p_{\mathrm{I},N}^{\mathrm{opt}} - \epsilon_N]^T$ as a feasible point for (5) with

$$\begin{aligned} \bar{\mathbf{p}}_{\mathrm{I},1}/\mathcal{L}_1 &= \min_{n=1,\ldots,N} \bar{\mathbf{p}}_{\mathrm{I},n}/\mathcal{L}_n \\ &= (p_{\mathrm{I},1}^{\mathrm{opt}} + \epsilon_1)/\mathcal{L}_1 \\ &> p_{\mathrm{I},1}^{\mathrm{opt}}/\mathcal{L}_1 \end{aligned}$$

implying that $\mathbf{p}_{\mathrm{I}}^{\mathrm{opt}}$ cannot be not the optimal solution of (5).

APPENDIX B: RATE FUNCTION APPROXIMATION

As a particular result of [21], the following inequality holds for all $(x, t) \in \mathbb{R}_+^2$ and $(\bar{x}, \bar{t}) \in \mathbb{R}_+^2$:

$$t \ln(1+x) \geq \bar{t} \ln(1+\bar{x}) \left(2 - \frac{\bar{t}}{t}\right) + \frac{\bar{t}\bar{x}}{1+\bar{x}} \left(1 - \frac{\bar{x}}{x}\right). \quad (20)$$

The following inequality holds for all $(x, y) \in \mathbb{R}_+^2, (\bar{x}, \bar{y}) \in \mathbb{R}_+^2$ [22]:

$$xy \leq \frac{\bar{x}\bar{y}}{4} \left(\frac{x}{\bar{x}} + \frac{y}{\bar{y}}\right)^2. \quad (21)$$

REFERENCES

[1] I. Krikidis, S. Timotheou, S. Nikolaou, G. Zheng, D. W. K. Ng, and R. Schober, "Simultaneous wireless information and power transfer in modern communication systems," *IEEE Commun. Mag.*, vol. 52, no. 11, pp. 104–110, Nov 2014.

[2] T. D. Ponnimbaduge Perera, D. N. K. Jayakody, S. K. Sharma, S. Chatzinotas, and J. Li, "Simultaneous wireless information and power transfer (SWIPT): Recent advances and future challenges," *IEEE Commun. Surveys Tuts.*, vol. 20, no. 1, pp. 264–302, Firstquarter 2018.

[3] L. Zhao, X. Wang, and K. Zheng, "Downlink hybrid information and energy transfer with massive MIMO," *IEEE Trans. Wireless Commun.*, vol. 15, no. 2, pp. 1309–1322, Feb. 2016.

[4] F. Zhu, F. Gao, Y. C. Eldar, and G. Qian, "Robust simultaneous wireless information and power transfer in beamspace massive MIMO," *IEEE Trans. Wireless Commun.*, pp. 1–1, 2019.

[5] K. Xu, Z. Shen, Y. Wang, X. Xia, and D. Zhang, "Hybrid time-switching and power splitting SWIPT for full-duplex massive MIMO systems: A beam-domain approach," *IEEE Trans. Veh. Technol.*, vol. 67, no. 8, pp. 7257–7274, Aug 2018.

[6] X. Wang and C. Zhai, "Simultaneous wireless information and power transfer for downlink multi-user massive antenna-array systems," *IEEE Trans. Commun.*, vol. 65, no. 9, pp. 4039–4048, Sep. 2017.

[7] G. Dong, H. Zhang, and D. Yuan, "Downlink achievable rate of massive MIMO enabled SWIPT systems over Rician channels," *IEEE Commun. Lett.*, vol. 22, no. 3, pp. 578–581, March 2018.

[8] A. Li and C. Masouros, "Energy-efficient SWIPT: From fully digital to hybrid analogdigital beamforming," *IEEE Trans. Veh. Technol.*, vol. 67, no. 4, pp. 3390–3405, April 2018.

[9] L. Zhao and X. Wang, "Massive MIMO downlink for wireless information and energy transfer with energy harvesting receivers," *IEEE Trans. Commun.*, vol. 67, no. 5, pp. 3309–3322, May 2019.

[10] J. Hu, K. Yang, G. Wen, and L. Hanzo, "Integrated data and energy communication network: A comprehensive survey," *IEEE Commun. Surveys Tuts.*, vol. 20, no. 4, pp. 3169–3219, Fourthquarter 2018.

[11] H. Sun, F. Zhou, R. Q. Hu, and L. Hanzo, "Robust beamforming design in a NOMA cognitive radio network relying on SWIPT," *IEEE J. Sel. Areas Commun.*, vol. 37, no. 1, pp. 142–155, Jan 2019.

[12] A. A. Nasir, H. D. Tuan, D. T. Ngo, T. Q. Duong, and H. V. Poor, "Beamforming design for wireless information and power transfer systems: Receive power-splitting vs transmit time-switching," *IEEE Trans. Commun.*, vol. 65, no. 2, pp. 876–889, 2017.

[13] D. Kudathanthirige, R. Shrestha, and G. A. Aruma Baduge, "Maxmin fairness optimal rate-energy trade-off of SWIPT for massive MIMO downlink," *IEEE Commun. Lett.*, vol. 23, no. 4, pp. 688–691, Apr. 2019.

[14] L. D. Nguyen, H. D. Tuan, T. Q. Duong, and H. V. Poor, "Beamforming and power allocation for energy-efficient massive MIMO," in *Proc. IEEE International Conference on DSP*, Aug 2017.

[15] A. A. Nasir, H. D. Tuan, T. Q. Duong, and M. Debbah, "NOMA throughput and energy efficiency in energy harvesting enabled networks," *IEEE Trans. Commun.*, 2019 (early access).

[16] P. Dong, H. Zhang, W. Xu, and G. Y. Li, "Coexistence of direct and relayed transmission users in multi-cell massive MIMO systems," *IEEE Trans. Veh. Technol.*, vol. 68, no. 4, pp. 3728–3746, April 2019.

[17] D. Peaucelle, D. Henrion, and Y. Labit, "Users guide for SeDuMi interface 1.03," 2002. [Online]. Available: http://homepages.laas.fr/peaucell/software/sdmguide.pdf

[18] B. R. Marks and G. P. Wright, "A general inner approximation algorithm for nonconvex mathematical programs," *Operations Research*, vol. 26, no. 4, pp. 681–683, 1978.

[19] Ö. Özdogan, E. Björnson, and E. G. Larsson, "Massive MIMO with spatially correlated Rician fading channels," *IEEE Trans. Commun.*, vol. 67, no. 5, pp. 3234–3250, May 2019.

[20] E. Björnson, J. Hoydis, and L. Sanguinetti, "Massive MIMO networks: Spectral, energy, and hardware efficiency," *Foundations and Trends in Signal Processing*, vol. 11, no. 3-4, pp. 154–655, 2017. [Online]. Available: http://dx.doi.org/10.1561/2000000093

[21] Z. Sheng, H. D. Tuan, T. Q. Duong, H. V. Poor, and Y. Fang, "Low-latency multiuser two-way wireless relaying for spectral and energy efficiencies," *IEEE Trans. Signal Process.*, vol. 66, no. 16, pp. 4362–4376, 2018.

[22] A. A. Nasir, H. D. Tuan, T. Q. Duong, and H. V. Poor, "UAV-enabled communication using NOMA," *IEEE Trans. Commun.*, vol. 67, no. 7, pp. 5126–5138, Jul. 2019.